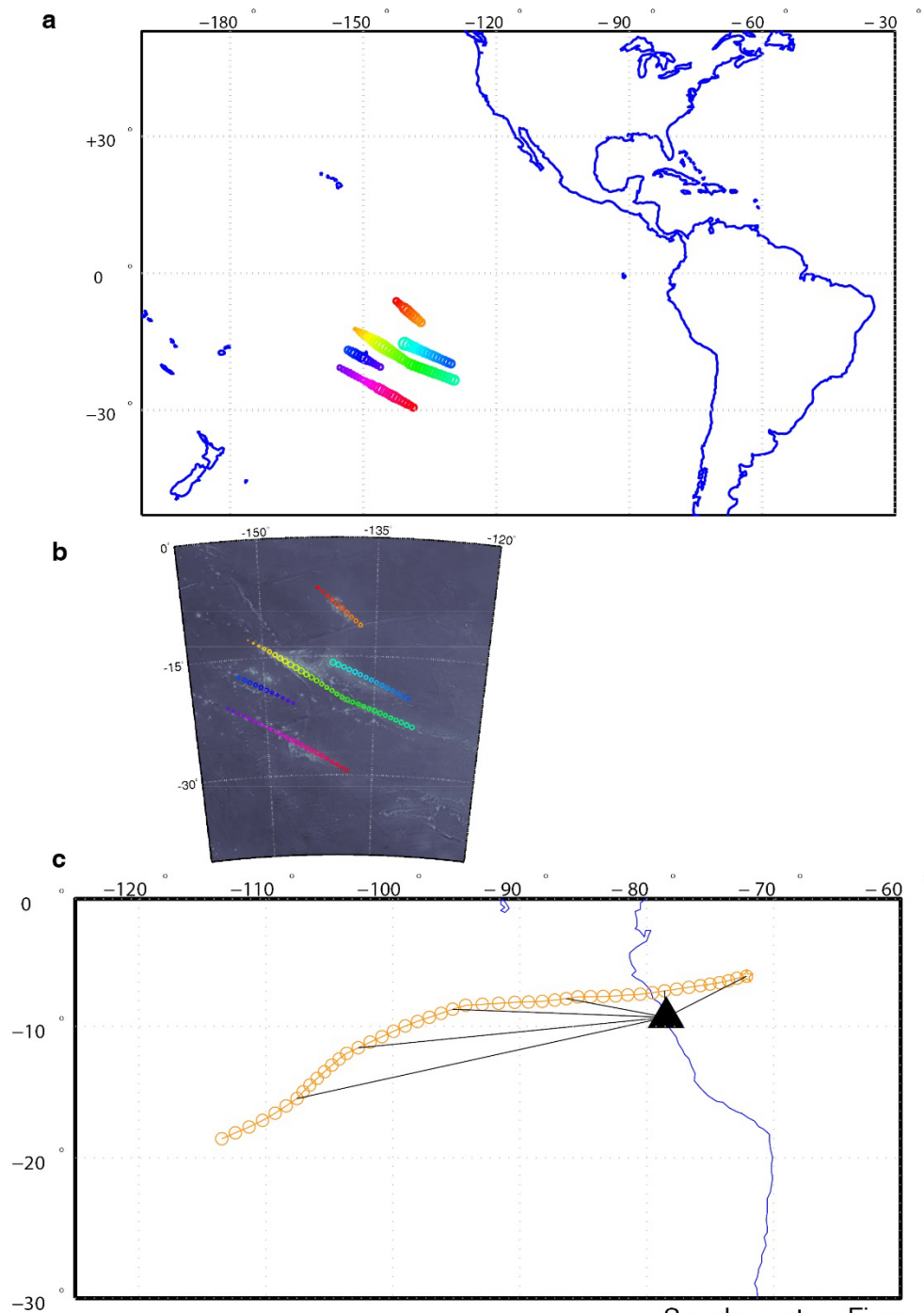


## SUPPLEMENT

### Supplementary Figure 1: Conjugate reconstructions

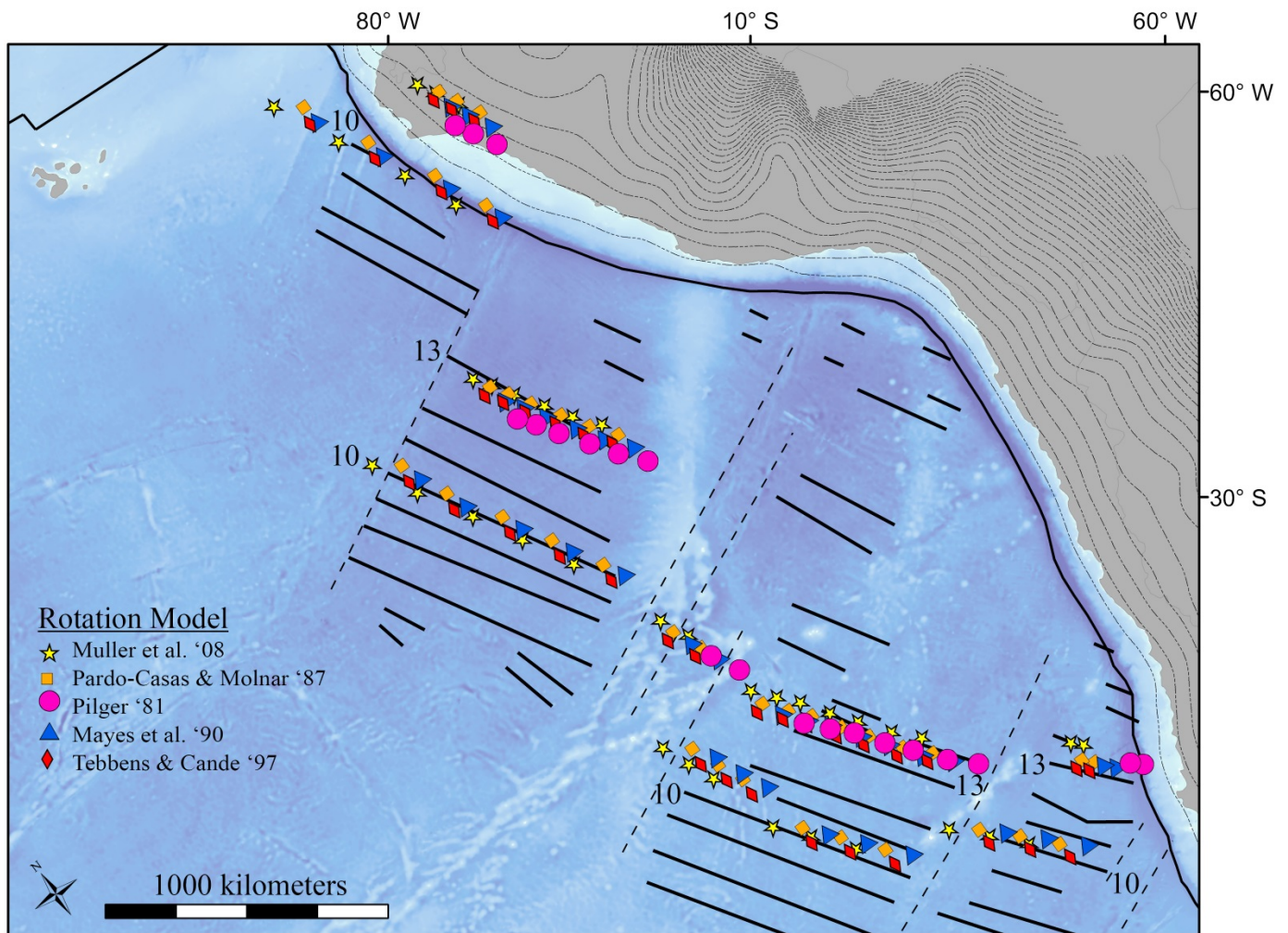
Panel a shows our 92 starting points on the Pacific. The color of the circle is used to match a starting point to a path in Figure 3. The size of the circle is relative to the crustal volume in a 100 km by 200 km swath centered on the starting point. Panel b shows the location of our starting points relative to Pacific bathymetry. Panel c shows our method of distance calculation used in Figure 3. Starting from the reconstructed conjugate point we rotate the point back in time in million year increments. We calculate a linear distance between each reconstructed point (orange circle) and the center of the flat slab (black triangle).



Supplementary Figure 1

## Supplementary Figure 2: Agreement of Reconstructions

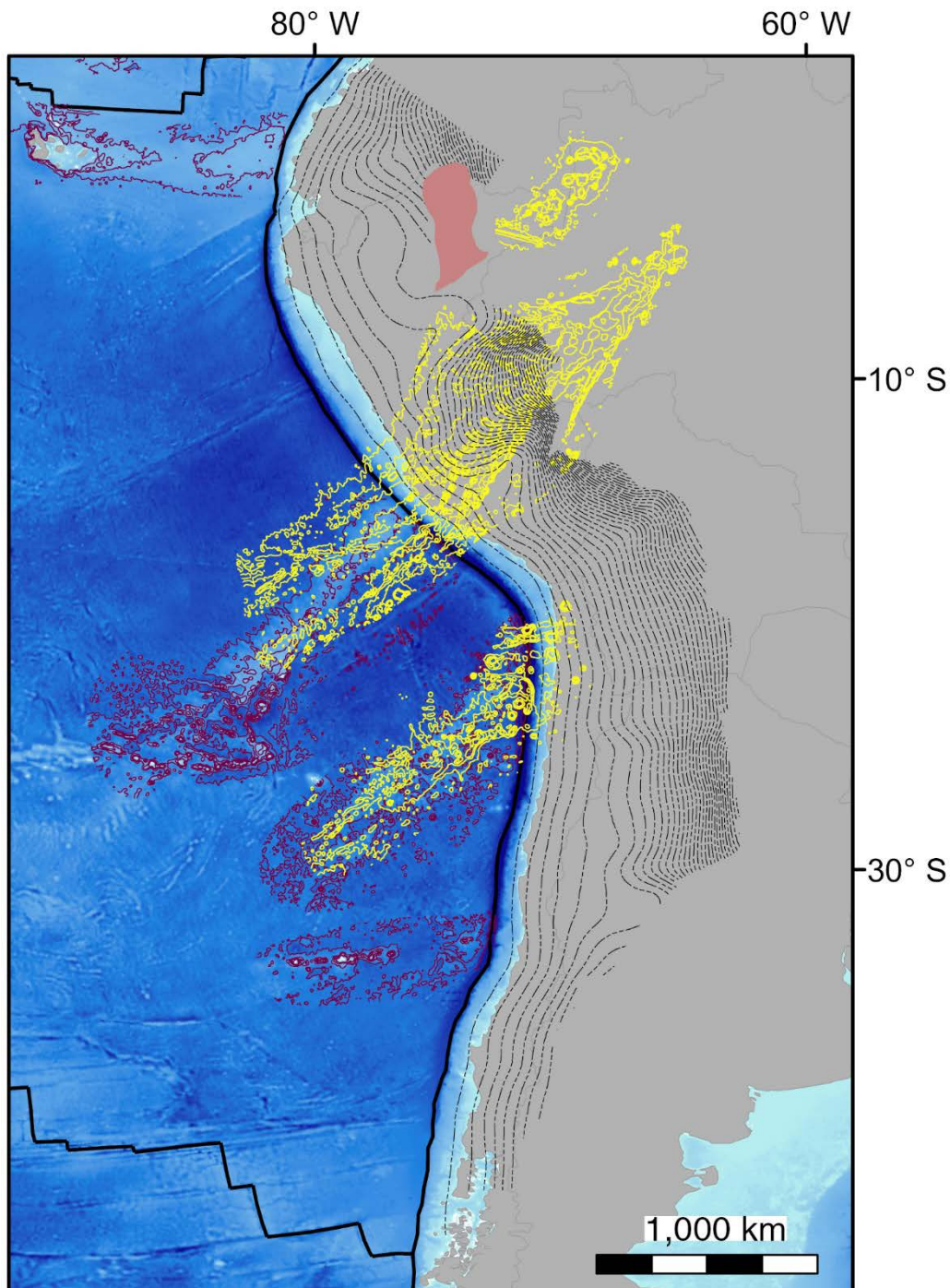
This map of the Nazca Plate shows the Pacific points of Figure 2 rotated by five different rotation models. We find that all models do an equally good job of predicting the location of magnetic isochrons as identified by Cande et al. (1989).



Supplementary Figure 2

### Supplementary Figure 3: Agreement of conjugate features

Map of present day South America depicting the agreement of our proposed conjugates with actual bathymetric features. The yellow lines are a mirror image of 1km contours of modern bathymetry on the Pacific plate. The purple lines are 1km contours of modern Nazca Plate bathymetry. Our proposed conjugates match well with the actual bathymetry. Our reconstruction of the Inca Plateau, however, is ~600 km to the east of the original location proposed by Gutscher et al. 1999.

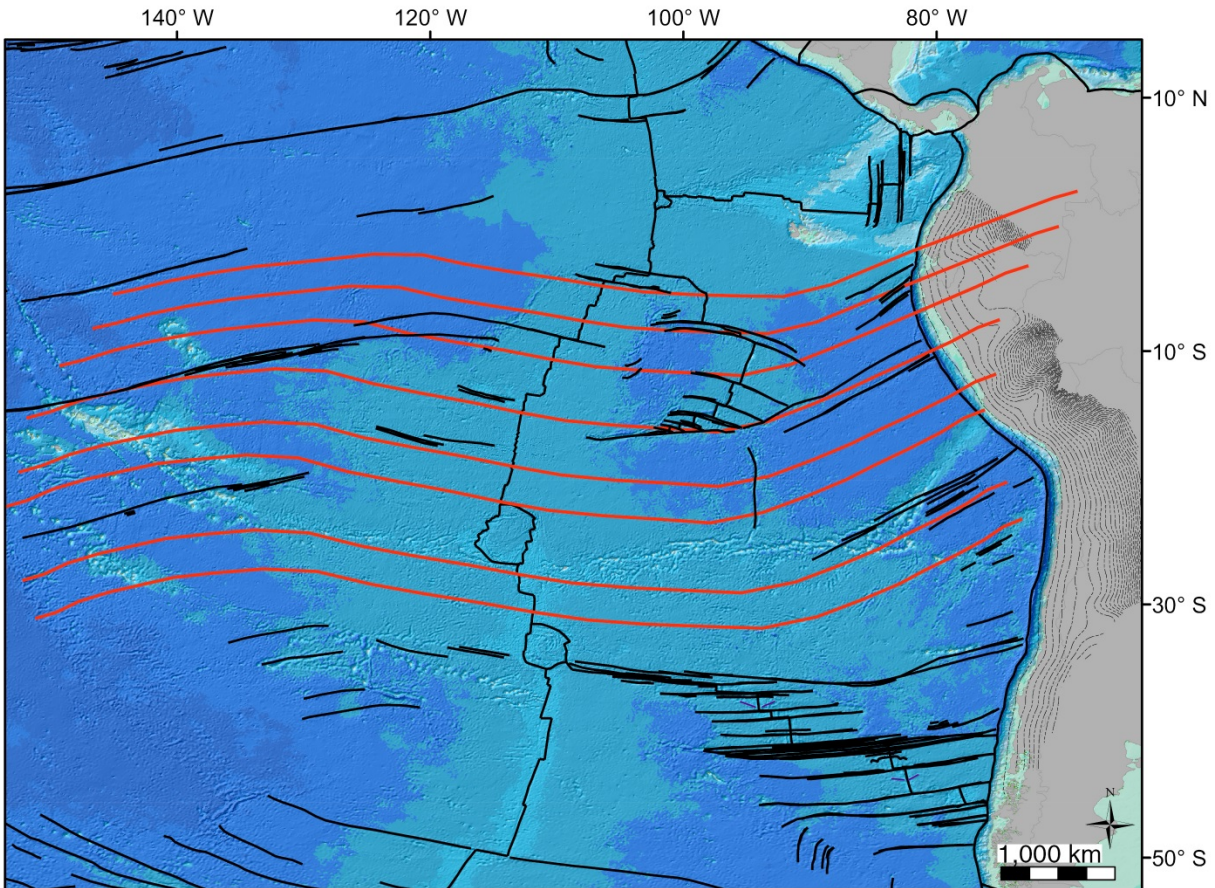


Supplementary Figure 3



#### Supplementary Figure 4: Agreement of fracture zones

This map shows synthetic fracture zones produced by the rotation model used in our reconstructions (Müller et al., 2008) in red and fracture zones as mapped by Matthews et al. (2011) in black. While it is unlikely that any model will be able to reproduce all of the complexities of fracture zones, we believe that this model does an excellent job at reproducing the large scale observable trends.



Supplementary Figure 4

### Supplementary Table 1

Poles of rotation for the Nazca plate relative to the Pacific plate used to test reconstructions of magnetic isochrons.

Chron	Latitude	Longitude	Angle	Source
13	68.71	-108.18	-49.44	(Müller et al., 2008)
13	69.85	-106.13	-49.54	(Pardo-Casas and Molnar, 1987)
13	69.04	-104.34	-49.63	(Mayes et al., 1990)
13	69.74	-105.82	-49.24	(Tebbens and Cande, 1997)
13	67.10	-102.40	-49.70	(Pilger, 1981)
10	67.01	-102.46	-43.14	(Müller et al., 2008)
10	67.34	-100.08	-43.77	(Pardo-Casas and Molnar, 1987)
10	66.20	-98.41	-44.05	(Mayes et al., 1990)
10	66.91	-98.30	-43.64	(Tebbens and Cande, 1997)

Supplementary Table 2

Poles of rotation for the Pacific and Nazca plates relative to the South America plate used in the reconstruction and tracking of conjugate features .

	Nazca/Farallon - South America			Pacific- South America		
Age (Ma)	Latitude	Longitude	Angle	Latitude	Longitude	Angle
1	-65.60	78.57	0.79	54.68	-79.97	0.69
2	-63.16	76.35	1.52	57.21	-77.37	1.44
3	62.58	-102.48	-2.28	57.94	-77.99	2.16
4	62.58	-99.95	-3.08	58.23	-79.94	2.82
5	62.56	-98.41	-3.88	58.40	-81.25	3.48
6	64.03	-98.60	-4.82	58.60	-82.11	4.14
7	64.34	-98.66	-5.82	59.44	-82.19	4.74
8	64.57	-98.67	-6.81	60.09	-82.30	5.34
9	64.68	-98.64	-7.81	60.67	-82.38	5.94
10	64.50	-98.21	-8.82	61.55	-82.60	6.52
11	64.25	-96.92	-9.86	62.66	-83.67	7.05
12	64.11	-96.34	-10.86	63.97	-83.70	7.58
13	64.10	-95.60	-11.89	65.02	-84.13	8.08
14	64.12	-94.86	-12.93	65.93	-84.69	8.57
15	64.14	-94.20	-13.97	66.74	-85.24	9.06
16	62.52	-93.88	-15.06	67.47	-85.77	9.55
17	61.12	-93.57	-16.16	68.14	-86.28	10.04
18	60.02	-93.26	-17.34	68.64	-86.92	10.44
19	59.15	-92.95	-18.61	69.02	-87.67	10.78
20	58.40	-92.59	-19.88	69.41	-88.61	11.10
21	59.16	-93.20	-21.14	69.53	-89.12	11.48
22	59.99	-93.89	-22.38	69.59	-89.53	11.86
23	60.73	-94.54	-23.64	69.65	-89.94	12.24
24	61.67	-96.53	-24.56	69.70	-90.34	12.63
25	62.57	-98.59	-25.36	69.56	-90.72	13.15
26	63.39	-100.60	-26.16	69.41	-91.23	13.67
27	64.20	-102.62	-27.00	69.16	-91.84	14.18
28	64.93	-104.89	-27.85	68.80	-91.95	14.67
29	65.49	-107.29	-28.71	68.54	-91.60	15.19
30	65.95	-109.69	-29.57	68.32	-91.13	15.71
31	66.33	-112.02	-30.44	68.11	-90.73	16.23
32	66.66	-114.29	-31.32	67.91	-90.39	16.75
33	66.92	-116.48	-32.20	67.73	-90.11	17.28
34	67.82	-119.85	-32.69	67.54	-87.92	17.77
35	68.51	-123.49	-33.21	67.49	-84.97	18.23
36	69.10	-127.23	-33.75	67.39	-82.23	18.70
37	69.59	-131.04	-34.31	67.23	-79.67	19.18
38	69.97	-134.88	-34.90	67.04	-77.32	19.67
39	70.25	-138.71	-35.46	66.86	-75.20	20.21
40	70.42	-142.51	-36.00	66.69	-73.30	20.79
41	70.58	-146.13	-36.90	66.49	-72.22	21.28
42	70.66	-149.60	-37.86	66.30	-71.30	21.76
43	70.80	-153.12	-38.91	65.97	-70.90	22.16
44	71.02	-156.70	-40.08	65.52	-71.11	22.44
45	71.23	-159.95	-41.23	65.26	-71.53	22.72
46	71.37	-163.08	-42.39	65.01	-71.96	23.00
47	71.35	-166.21	-43.60	64.57	-72.08	23.29
48	71.25	-169.36	-44.84	64.03	-72.15	23.56
49	71.21	-173.79	-45.93	63.24	-72.73	23.74
50	71.06	-177.97	-47.05	62.46	-73.29	23.93
51	70.84	178.11	-48.19	61.69	-73.84	24.12
52	70.60	174.43	-49.31	61.06	-74.60	24.32
53	70.29	170.95	-50.37	60.52	-75.43	24.60
54	69.66	167.67	-51.42	59.69	-75.85	25.05
55	68.90	164.68	-52.47	58.80	-76.18	25.58
56	68.15	162.15	-53.50	57.98	-76.54	26.12
57	67.62	161.04	-54.02	57.47	-77.10	26.68
58	67.09	160.00	-54.55	56.97	-77.64	27.24
59	66.57	159.04	-55.08	56.50	-78.15	27.80
60	66.05	158.15	-55.61	56.05	-78.64	28.37
61	65.53	157.32	-56.15	55.62	-79.12	28.93
62	64.93	156.69	-56.67	55.20	-79.33	29.58
63	64.33	156.13	-57.19	54.80	-79.52	30.23
64	63.65	155.89	-58.09	53.82	-79.08	30.71
65	62.99	155.71	-59.05	52.79	-78.63	31.18
66	62.39	155.50	-59.98	51.88	-78.32	31.65
67	61.86	155.25	-60.86	51.11	-78.19	32.10
68	61.35	155.05	-61.79	50.34	-78.06	32.55
69	60.84	154.94	-62.82	49.52	-77.88	33.01
70	60.35	154.83	-63.85	48.72	-77.74	33.48
71	59.87	154.74	-64.88	47.95	-77.62	33.96
72	59.48	154.59	-65.99	47.14	-77.61	34.34
73	59.22	154.36	-67.19	46.28	-77.74	34.56
74	58.96	154.21	-68.27	45.62	-77.84	34.85
75	58.71	154.17	-69.16	45.25	-77.86	35.21
76	58.37	154.09	-70.06	44.83	-77.93	35.66
77	57.87	154.06	-70.74	44.64	-77.99	36.38
78	57.33	154.07	-71.33	44.57	-78.03	37.18
79	56.80	154.09	-71.91	44.52	-78.08	37.99
80	56.31	154.09	-72.40	44.61	-78.21	38.79

Supplementary Table 3

The starting points on the Pacific plate (Latitude1, Longitude1), seafloor age, crustal volume in a swath cenered on the starting point, and our reconstructed conjugate point on the Nazca plate (Latitude2, Longitude2).

Point	Latitude1	Longitude1	Age (Ma)	Volume (km <sup>3</sup> )	Latitude2	Longitude2
1	-6.30	-142.53	60.72	1,896.87	2.07	-65.81
2	-6.83	-141.92	57.63	2,143.89	1.06	-67.33
3	-7.36	-141.31	54.98	2,474.92	-0.02	-68.80
4	-7.89	-140.70	54.20	4,506.24	-0.76	-68.92
5	-8.42	-140.08	52.91	5,118.10	-1.66	-69.51
6	-8.95	-139.47	51.24	4,610.92	-2.70	-70.44
7	-9.47	-138.86	50.71	4,527.80	-3.33	-70.27
8	-10.00	-138.25	48.74	4,410.06	-4.47	-71.42
9	-10.53	-137.63	47.69	3,406.44	-5.30	-71.77
10	-11.06	-137.02	46.86	3,339.93	-6.08	-72.12
11	-12.55	-151.84	90.20	311.42	-0.24	-52.67
12	-12.98	-151.15	87.24	867.60	-0.84	-54.29
13	-13.40	-150.46	84.52	1,971.65	-1.45	-55.69
14	-13.83	-149.77	83.65	3,063.49	-1.97	-55.69
15	-14.25	-149.08	65.43	3,372.65	-5.33	-68.74
16	-14.68	-148.39	64.07	4,516.95	-5.96	-68.96
17	-15.10	-147.71	62.27	5,970.24	-6.68	-69.46
18	-15.53	-147.02	61.99	7,391.30	-7.12	-68.95
19	-15.95	-146.33	59.63	8,192.43	-7.94	-69.81
20	-16.38	-145.64	53.99	8,276.48	-9.73	-73.17
21	-16.80	-144.95	52.95	7,528.97	-10.49	-73.33
22	-17.23	-144.26	51.17	6,676.92	-11.54	-74.08
23	-17.65	-143.57	50.44	5,924.89	-12.16	-73.95
24	-18.08	-142.88	49.73	5,120.90	-12.77	-73.79
25	-18.51	-142.20	47.70	4,416.13	-13.92	-74.74
26	-18.93	-141.51	45.59	4,467.57	-15.22	-76.46
27	-19.36	-140.82	44.04	3,500.96	-16.26	-77.50
28	-19.78	-140.13	42.56	3,400.41	-17.27	-78.44
29	-20.20	-139.44	40.97	4,396.92	-18.33	-79.50
30	-20.51	-138.71	39.66	4,620.93	-19.07	-80.06
31	-20.77	-137.94	39.41	4,176.71	-19.24	-79.47
32	-21.04	-137.18	38.74	4,293.07	-19.55	-79.22
33	-21.30	-136.41	30.90	4,371.58	-23.02	-86.12
34	-21.56	-135.65	30.51	4,202.19	-23.26	-85.84
35	-21.83	-134.88	29.90	4,666.64	-23.63	-85.88
36	-22.09	-134.12	28.84	4,791.35	-24.26	-86.55
37	-22.36	-133.35	28.14	4,048.29	-24.68	-86.72
38	-22.62	-132.59	27.70	4,337.69	-24.96	-86.51
39	-22.89	-131.82	26.15	4,328.27	-25.86	-87.89
40	-23.15	-131.06	25.06	4,632.29	-26.50	-88.62
41	-23.42	-130.29	24.64	4,742.64	-26.78	-88.39
42	-23.68	-129.53	24.30	4,816.57	-27.01	-88.04
43	-15.78	-140.66	44.74	7,521.73	-12.38	-77.30
44	-16.06	-139.92	43.51	6,392.49	-13.12	-77.98
45	-16.38	-139.17	42.65	5,453.62	-13.70	-78.21
46	-16.69	-138.42	41.20	5,428.23	-14.58	-79.12
47	-17.01	-137.68	40.31	4,691.05	-15.17	-79.37
48	-17.32	-136.93	37.01	4,368.34	-16.57	-81.51
49	-17.64	-136.19	35.74	4,503.07	-17.17	-81.80
50	-17.96	-135.44	35.45	3,848.80	-17.38	-81.24
51	-18.27	-134.70	34.57	3,859.25	-17.81	-81.18
52	-18.59	-133.95	34.24	4,053.60	-18.03	-80.66
53	-18.90	-133.21	33.15	3,776.03	-18.52	-80.77
54	-19.22	-132.46	31.71	3,292.75	-19.42	-81.91
55	-19.54	-131.72	30.50	3,427.94	-20.20	-82.77
56	-19.85	-130.97	29.72	3,424.29	-20.73	-83.04
57	-20.17	-130.23	28.55	3,199.58	-21.48	-83.85
58	-17.21	-153.38	87.22	2,713.57	-4.85	-56.85
59	-17.57	-152.66	86.81	3,462.03	-5.30	-56.47
60	-17.94	-151.94	83.98	4,228.75	-5.94	-57.76
61	-18.30	-151.22	83.20	3,778.29	-6.42	-57.64
62	-18.67	-150.50	80.54	4,296.81	-7.20	-58.95
63	-19.04	-149.78	75.74	4,449.34	-8.32	-61.84
64	-19.40	-149.05	70.66	3,250.28	-9.55	-64.90
65	-19.77	-148.33	68.12	2,212.25	-10.36	-66.06
66	-20.14	-147.61	66.35	1,807.90	-11.01	-66.53
67	-20.50	-146.89	63.21	1,509.98	-11.88	-67.83
68	-20.87	-146.17	61.90	1,614.69	-12.44	-67.95
69	-21.01	-155.29	89.66	1,124.26	-8.26	-57.39
70	-21.38	-154.57	88.38	1,339.42	-8.80	-57.58
71	-21.74	-153.84	87.88	1,465.25	-9.27	-57.26
72	-22.11	-153.12	86.30	1,772.32	-9.83	-57.62
73	-22.48	-152.40	85.17	1,732.23	-10.34	-57.69
74	-22.84	-151.68	84.09	1,732.48	-10.84	-57.70
75	-23.21	-150.96	83.12	1,596.97	-11.34	-57.68
76	-23.57	-150.23	78.37	1,244.54	-12.43	-60.44
77	-23.94	-149.51	77.58	1,868.85	-12.94	-60.34
78	-24.31	-148.79	72.84	1,882.21	-14.07	-63.05
79	-24.67	-148.07	69.95	3,268.23	-14.93	-64.41
80	-25.04	-147.35	68.98	2,755.02	-15.46	-64.42
81	-25.40	-146.62	60.46	4,580.50	-17.24	-69.05
82	-25.77	-145.90	58.72	4,748.05	-17.88	-69.40
83	-26.14	-145.18	56.25	4,079.82	-18.64	-70.18
84	-26.50	-144.46	54.10	3,879.73	-19.66	-70.93
85	-26.87	-143.74	49.80	4,638.09	-21.55	-73.10
86	-27.23	-143.02	48.71	4,960.79	-22.22	-73.06
87	-27.60	-142.29	48.09	3,962.24	-22.71	-72.71
88	-27.97	-141.57	45.53	3,253.91	-24.10	-74.60
89	-28.33	-140.85	43.03	3,112.10	-25.51	-76.48
90	-28.70	-140.13	40.01	3,037.82	-27.19	-78.83
91	-29.06	-139.41	38.52	2,380.76	-27.91	-79.12
92	-29.43	-138.68	37.72	2,487.10	-28.37	-78.89

## References

- Cande, S.C., LaBrecque, J.L., Larson, R.L., Pittman, W.C., Golovchenko, X., Haxby, W.F., 1989. Magnetic lineations of the world's ocean basins, Magnetic lineations of the world's ocean basins. AAPG, Tulsa, OK.
- Matthews, K.J., Müller, R.D., Wessel, P., Whittaker, J.M., 2011. The tectonic fabric of the ocean basins. *Journal of Geophysical Research: Solid Earth* 116, B12109.
- Mayes, C.L., Lawver, L.A., Sandwell, D.T., 1990. Tectonic History and New Isochron Chart of the South Pacific. *J. Geophys. Res.* 95, 8543-8567.
- Müller, R.D., Sdrolias, M., Gaina, C., Roest, W.R., 2008. Age, spreading rates, and spreading asymmetry of the world's ocean crust, *Geochemistry Geophysics Geosystems*. American Geophysical Union, p. Q04006.
- Pardo-Casas, F., Molnar, P., 1987. Relative motion of the Nazca (Farallon) and South American Plates since Late Cretaceous time. *Tectonics* 6, 233-248.
- Pilger, R.H., 1981. Plate Reconstructions, Aseismic Ridges, and Low-Angle Subduction beneath the Andes. *Geological Society of America Bulletin* 92, 448-456.
- Tebbens, S.F., Cande, S.C., 1997. Southeast Pacific tectonic evolution from early Oligocene to present. *Journal of Geophysical Research* 102, 12061-12084.